



Controlled synthesis of uniform ultrafine CuO nanowires as anode material for lithium-ion batteries

Fei Wang*, Weizhe Tao, Mingshu Zhao, Minwei Xu, Shengchun Yang, Zhanbo Sun, Liqun Wang, Xiaoping Song**

MOE Key Laboratory for Non-equilibrium Synthesis and Modulation of Condensed Matter, School of Science, Xi'an Jiaotong University, Xi'an 710049, PR China

ARTICLE INFO

Article history:

Received 24 May 2011

Received in revised form 18 July 2011

Accepted 30 July 2011

Available online 4 August 2011

Keywords:

Copper oxide

Ultrafine nanowires

Anode

Lithium-ion battery

ABSTRACT

A simple solution route is used to synthesize ultrafine Cu(OH)₂ nanowires by restraining the morphology transformation of early formed 1D nanostructure. The obtained ultrafine nanowires can be well preserved at a low temperature structure transformation in solid state. As anode material for lithium-ion batteries, the ultrafine CuO nanowires exhibit high reversible capacity, superior cycling performance and improved rate capability. The improved electrochemical properties of CuO nanowires are ascribed to their ultrafine size which lead to the reduced over-potential, extra reversible reactions at low potentials and improved interface performance between the electrode and electrolyte.

© 2011 Elsevier B.V. All rights reserved.

1. Introduction

Lithium-ion batteries (LIBs) are widely used in portable electronic equipments. Now, they are becoming a good choice for electric vehicles and hybrid electrical vehicles, but their performance still lies behind the increasing demands of the consumer. It's necessary to explore new electrode materials or design novel nanostructures of electrode materials to meet these demands [1–6]. Recently, nano-sized transition metal oxides (MO, where M is Fe, Co, Ni, and Cu) have been widely investigated as promising anodes for LIBs since they were first reported by Tarascon et al. [2]. Among them, copper oxide (CuO) has attracted much attention due to its high theoretical capacity (670 mAh g⁻¹), non-toxic, low cost and facile synthesis. However, the severe volume expansion/contraction during lithiation/delithiation causes the pulverization of electrodes and leads to rapid deterioration in capacity. To overcome this intrinsic drawback, an effective approach is adopted to fabricate CuO/C nano-composites [7–13]. The carbon materials used in composites can not only improve the electronic conductivity but also prevent the breakdown of electrode materials during Li⁺ insertion and extraction [8]. Nevertheless, this strategy usually sacrifices the reversible capacity of CuO due to the introduction of carbon. Moreover, the reliable and

facile synthesis is still a challenge for well-designed CuO/C nano-composites.

Because the electrochemical properties of CuO can be greatly affected by morphologies, intensive research has focused on the controlled synthesis of various CuO nanostructures over the past several years [14–23]. Improved cycling performance has been obtained in most of them. However, it is still a great challenge to achieve high rate capability in pure CuO nanostructures. In general, it is well accepted that a smaller size of CuO can lead to higher capacity and higher rate capability. This reduces the over-potential and allows faster reaction kinetics at the electrode surface [5]. Therefore, the synthesis of CuO nanostructures with ultrafine size is a promising approach to obtain improved rate capability in pure CuO nanostructures.

Polycrystalline CuO nanowires with tens of nanometers in diameter have been investigated by others as anode materials for LIBs, which exhibited superior cycling performance [15]. In this paper, we focused on the controlled synthesis of uniform CuO nanowires with ultrafine size and good dispersion by a simple solution route [24–28], and investigated their lithium storage capacity, rate capability as well as cycling performance for LIB anode materials.

2. Experimental

In a typical experiment, 0.2 mol NaOH was dissolved in 100 ml distilled water and 1 mmol CuCl₂·2H₂O was dissolved in 10 ml distilled water. Then, the CuCl₂ solution was dropwise added into the NaOH solution under magnetic stirring at 20 °C. After reaction for 20 min, the mixed solution turned turbid. The blue products were harvested by high-speed centrifugation and thoroughly washed with distilled water and ethanol. The obtained blue precipitates were dried in oven for 2 h at 60 °C.

* Corresponding author. Tel.: +86 29 82663034; fax: +86 29 82667872.

** Corresponding author. Tel.: +86 29 82665892; fax: +86 29 82667872.

E-mail addresses: feiwang@mail.xjtu.edu.cn (F. Wang), xpsong@mail.xjtu.edu.cn (X. Song).

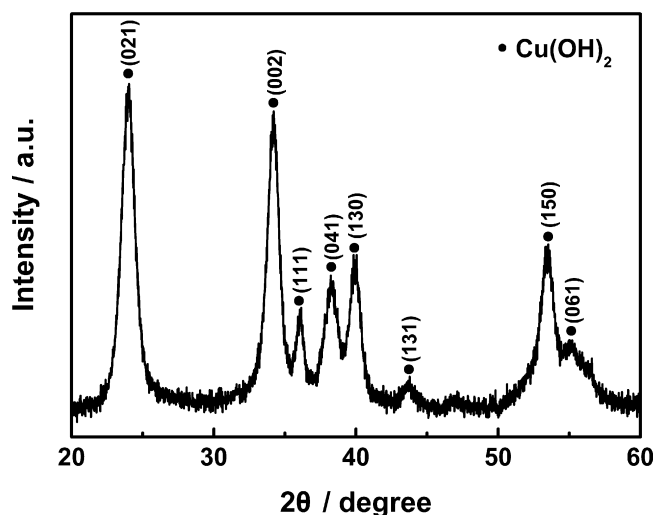


Fig. 1. XRD pattern of ultrafine $\text{Cu}(\text{OH})_2$ nanowires.

Finally, the dried powders were heat-treated in a furnace for 2 h at 150°C . In addition, the turbid solution mentioned above was heat-treated in water bath at 75°C for 15 min. The black precipitates were harvested and dried.

The structure and morphology of the products were characterized by X-ray diffraction (XRD, Bruke D8-Advance, $\text{Cu-K}\alpha$, $\lambda = 0.15406\text{ nm}$), field emission scanning electron microscope (FESEM, JEOL JSM-7100F) and transmission electron microscopy (TEM, JEOL JEM-2100).

Electrochemical properties of CuO electrodes were tested using two-electrode Swagelok cells with lithium metal as the counter and reference electrodes. The working electrodes consisted of 70 wt.% active materials (CuO), 20 wt.% conductive material (acetylene black), and 10 wt.% binder (polyvinylidene fluoride, PVDF). The electrolyte was 1 M LiPF_6 in a mixture of 50 vol.% ethylene carbonate (EC) and 50 vol.% diethylene carbonate (DEC). Test cells were assembled in argon filled glove box. The galvanostatical charge–discharge measurement was carried out by using an Arbin BT2000 battery testing system in the voltage range of 0.02–3.0 V (vs. Li/Li^+). The cyclic voltammograms (CV) were tested on Ametek VMC-4 electrochemical testing system at a scan rate of 0.2 mV s^{-1} between 0 V and 3.0 V (vs. Li/Li^+).

3. Results and discussion

The XRD pattern of the sample prepared by using 1 mmol $\text{CuCl}_2 \cdot 2\text{H}_2\text{O}$ and the reaction time of 20 min (see Section 2) is shown in Fig. 1. All the diffraction peaks are well consistent with the orthorhombic $\text{Cu}(\text{OH})_2$ (JCPDS No. 13-0420). The relatively broad diffraction peaks indicate the small crystallite size

for the sample. Fig. 2a and b presents the typical SEM and TEM images of as-prepared $\text{Cu}(\text{OH})_2$ nanostructure, which show the uniform ultrafine nanowires with about 5 nm (the inset HRTEM of Fig. 2b) in diameter and several hundreds nanometers in length. The nanowires exhibit good dispersion in spite of a slight aggregation due to their high surface energy.

The reactions occurred in the solution of NaOH and CuCl_2 can be summarized as Eqs. (1) and (2). In highly basic solution, Cu^{2+} prefers square planar coordination by OH^- to form $[\text{Cu}(\text{OH})_4]^{2-}$ instead of $\text{Cu}(\text{OH})_2$ precipitates. The nucleation of $\text{Cu}(\text{OH})_2$ should start from localized regions with relatively high concentrations of $[\text{Cu}(\text{OH})_4]^{2-}$. Once the nucleus are formed, 1D $\text{Cu}(\text{OH})_2$ nanostructure are easily formed because the growth along [1 0 0] direction is much faster than other directions [24,29]. Whereas, the 1D $\text{Cu}(\text{OH})_2$ nanostructures are unstable in basic solution, which can transform to 2D nanostructures through the coordination of OH^- to d_z^2 of Cu^{2+} and further transform to 3D nanostructures by weak hydrogen bond interactions [29]. In this research, to obtain ultrafine $\text{Cu}(\text{OH})_2$ nanowires, the Cu^{2+} concentration and reaction time were strictly controlled to restrain the transformation of 1D nanostructures formed in early stage. From Fig. 3 we can see clearly that both prolonging the reaction time and increasing the Cu^{2+} concentration can lead to two-dimensional aggregation growth.



To investigate the electrochemical properties of ultrafine nanowires as anode materials for LIBs, the as-prepared ultrafine $\text{Cu}(\text{OH})_2$ nanowires should be transformed to CuO structure without obvious morphological changes. Fig. 4a shows the SEM image of the sample heat-treated at 150°C for 2 h. The morphology of ultrafine nanowires is well preserved. XRD pattern (Fig. 4c) shows that the crystal structure is transformed to monoclinic CuO (JCPDS No. 05-0661). The weak and broad diffraction peaks indicate the fine grains of CuO. By using the Scherrer's formula and the full width at half maximum (FWHM) data of (1 1 1) peak, the mean crystallite size of CuO nanowires can be calculated to be 3.7 nm. For comparison, the ultrafine $\text{Cu}(\text{OH})_2$ nanowires were also heat-treated in the solution at 75°C for 15 min. Bowknot-like products (Fig. 4b) are obtained instead of ultrafine nanowires. From XRD pattern (Fig. 4d) we can see that the products are also monoclinic CuO. As is well known, $\text{Cu}(\text{OH})_2$ is a metastable phase which easily transforms into more stable CuO in both solid state and solution. Although the

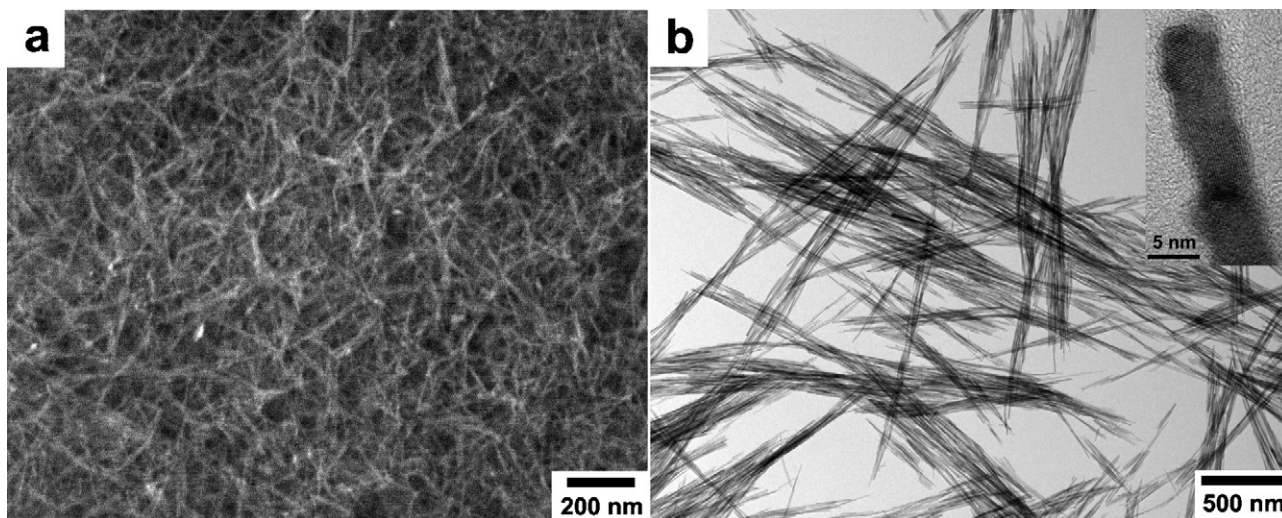


Fig. 2. SEM image (a) and TEM image (b) of ultrafine $\text{Cu}(\text{OH})_2$ nanowires. The inset of (b) is the HRTEM image of ultrafine $\text{Cu}(\text{OH})_2$ nanowires.

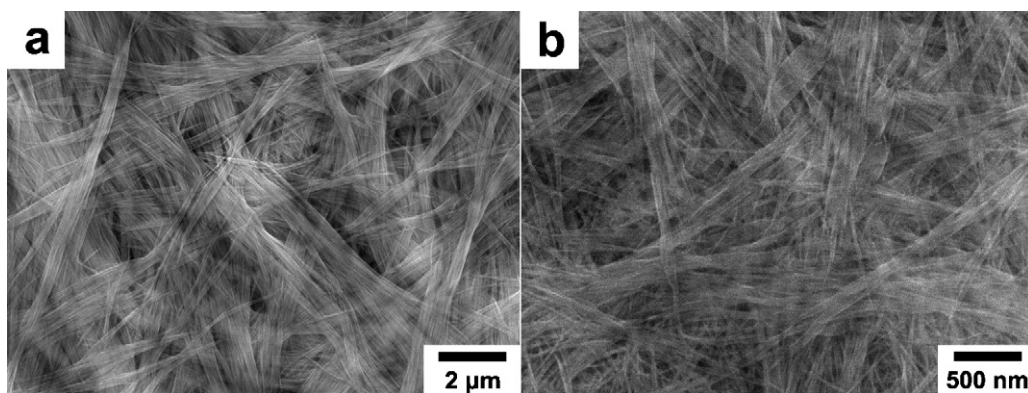


Fig. 3. (a) SEM image of $\text{Cu}(\text{OH})_2$ nanostructure prepared by using 1 mmol $\text{CuCl}_2 \cdot 2\text{H}_2\text{O}$ and the reaction time of 3 h; (b) SEM image of $\text{Cu}(\text{OH})_2$ nanostructure prepared by using 4 mmol $\text{CuCl}_2 \cdot 2\text{H}_2\text{O}$ and the reaction time of 20 min.

main feature of two different routes is the formation of square planar entities CuO_4 giving rise to CuO [28,30], the morphology changes are quite different. There is a little change in solid transformation but a great change in solution which associated with the formation of sheet-like structure and further self-assembling into bowknot-like architectures through an oriented aggregate mechanism [31].

Fig. 5a and b shows the first two CV curves of ultrafine CuO nanowires and bowknot-like CuO at a scan rate of 0.2 mV s^{-1} . Two kinds of CuO electrodes show similar cathodic and anodic peaks in whole scan processes, but some differences can also be found between them. Compared to the bowknot-like CuO , the cathodic peaks of the ultrafine CuO nanowires locate at relatively high potentials and anodic peaks locate at relatively low poten-

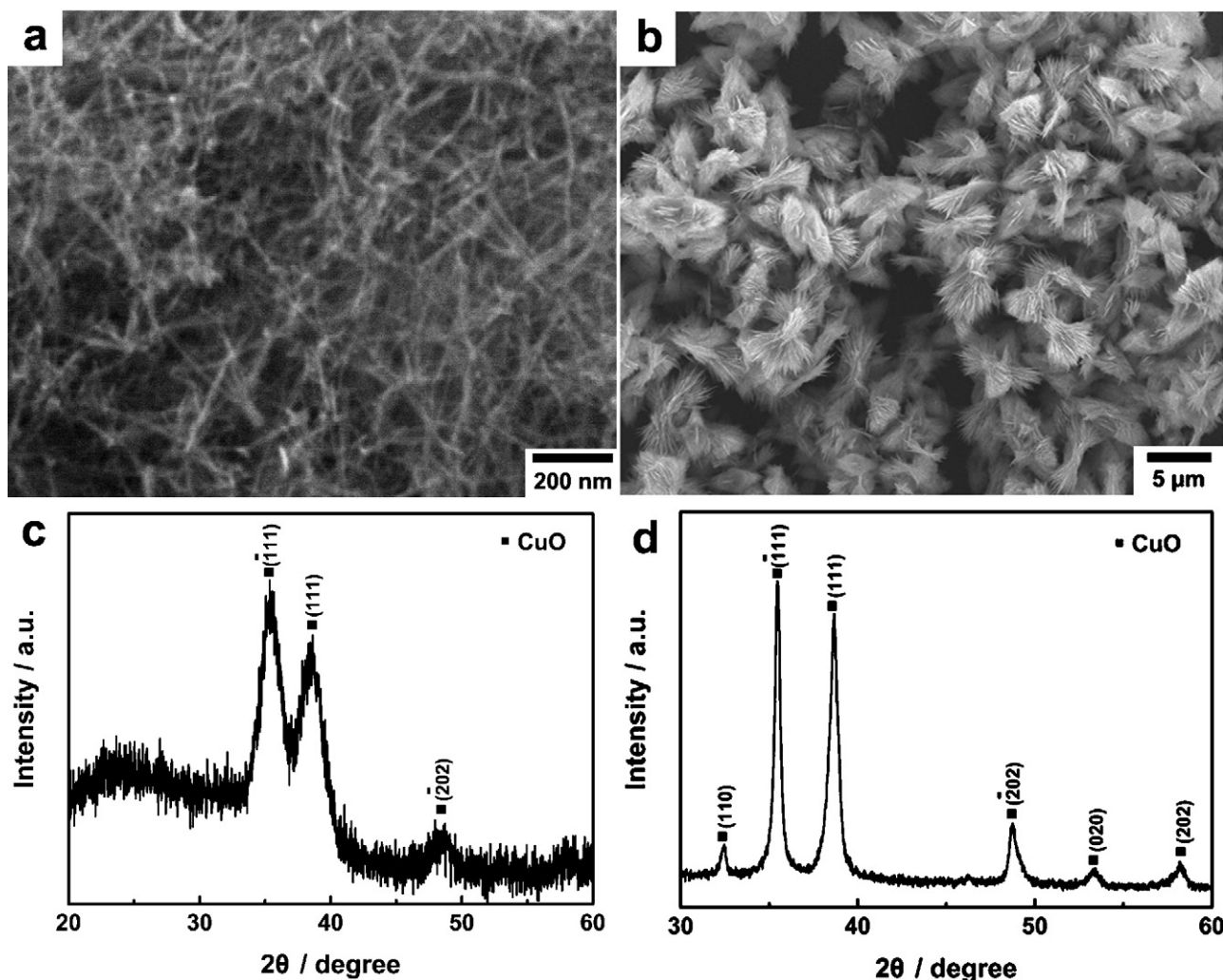


Fig. 4. SEM images of ultrafine CuO nanowires (a) and bowknot-like CuO (b); XRD patterns of ultrafine CuO nanowires (c) and bowknot-like CuO (d).

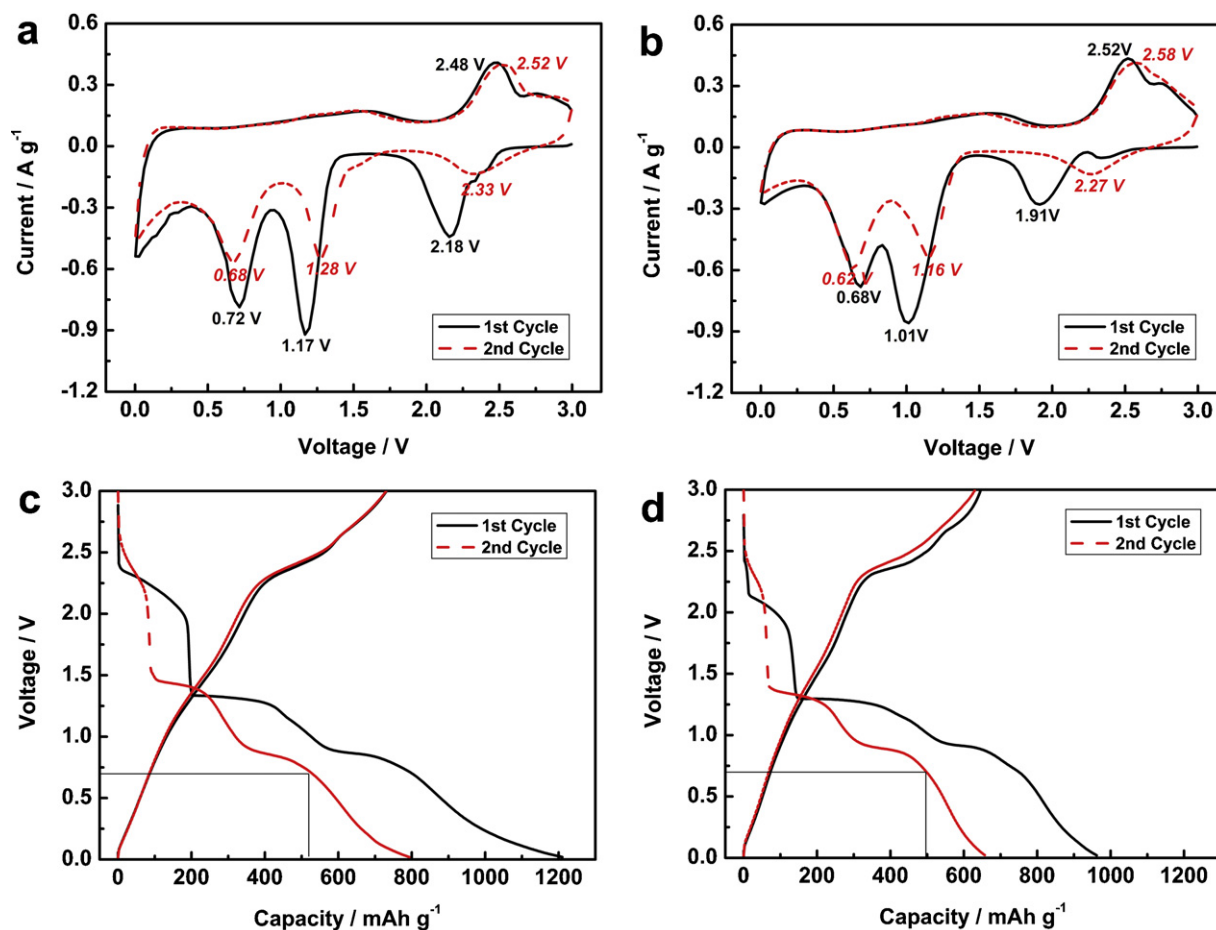


Fig. 5. CV curves of ultrafine CuO nanowires (a) and bowknot-like CuO (b); voltage–capacity curves of ultrafine CuO nanowires (c) and bowknot-like CuO (d).

tials. The potential difference between the cathodic and anodic peaks can be considered as the polarization of the electrode. The reduced over-potential in ultrafine CuO nanowires shows faster reaction kinetics. The large surface areas of ultrafine CuO nanowires make the Li^+ insertion/extraction take place mostly at the surface rather than in the bulk, which greatly reduce the Li^+ diffusion distance. Hence, the electrochemical reaction of lithium is easily achieved in the ultrafine CuO nanowires. Furthermore, a relatively strong cathodic peak at low potentials near 0V can be found in the ultrafine CuO nanowires electrode. The cathodic peak at low potentials can lead to an extra capacity besides the reversible Li-driven decomposition of the transition-metal oxide, which should be associated with the formation of a gel-like film on the surface of oxides particles. The formation and dissolution of gel-like film was proposed as being the result of a catalytically enhanced electrolyte reduction [32]. Therefore, the ultrafine CuO nanowires should exhibit better catalytic effect and thus achieve a higher reversible capacity at low potentials. Fig. 5c and d shows the first two voltage–capacity curves of ultrafine CuO nanowires and bowknot-like CuO at 0.1 C ($1\text{ C} = 670\text{ mA g}^{-1}$). The discharge capacity of ultrafine CuO nanowires in the second cycle can achieve 790 mAh g^{-1} , while it is only 660 mAh g^{-1} for bowknot-like CuO. From black straight line marked in Fig. 5c and d we can see that the capacity difference between two kinds of CuO electrodes mainly locates below 0.7V, which is corresponding well with the CV results.

The cycling performances of the two CuO electrodes at 0.1 C are illustrated in Fig. 6a and b. The discharge capacities at 30th cycle

are 680 and 470 mAh g^{-1} , respectively. Increasing the current density to 0.3 C, the discharge capacity of ultrafine CuO nanowires can also be maintained at about 660 mAh g^{-1} after 70 cycles (Fig. 6c). Improved cycling performance of CuO nanowires can be attributed to the ultrafine size and good dispersion which is beneficial for accommodating the strain associated with the severe volume variations during Li^+ insertion and extraction. Fig. 6d shows the rate capability of two kinds of CuO electrodes at different current densities. Compared with bowknot-like CuO, the ultrafine CuO nanowires exhibit higher rate performance. It can be observed that a charge capacity of about 760 mAh g^{-1} is obtained at 0.1 C after 10 cycles, and this value is slowly reduced to 730 mAh g^{-1} , 680 mAh g^{-1} , 590 mAh g^{-1} , 420 mAh g^{-1} at 0.2 C, 0.4 C, 0.8 C and 1.6 C, respectively. Furthermore, the charge capacity can return to the original value and gradually increase after 50 cycles when the current density turns back to 0.1 C. The improved rate capability indicates a fast transferring of electrons and Li^+ in ultrafine CuO nanowires because of their large electrode–electrolyte contact area and shortened Li^+ diffusion distance. The gradual increase of the excess capacity after 50 cycles should be attributed that not all surface, such as the internal surface between the nanowires, is covered with polymer layer after several cycles at relatively rapid charge–discharge process. Shaju et al. [33] have suggested that the growth of polymer layer on the internal surface is limited to some extent because of slower mass transport of the constituents that make up the polymer layer. Therefore, the polymer layer on internal surface builds-up slowly, over a number of cycles.

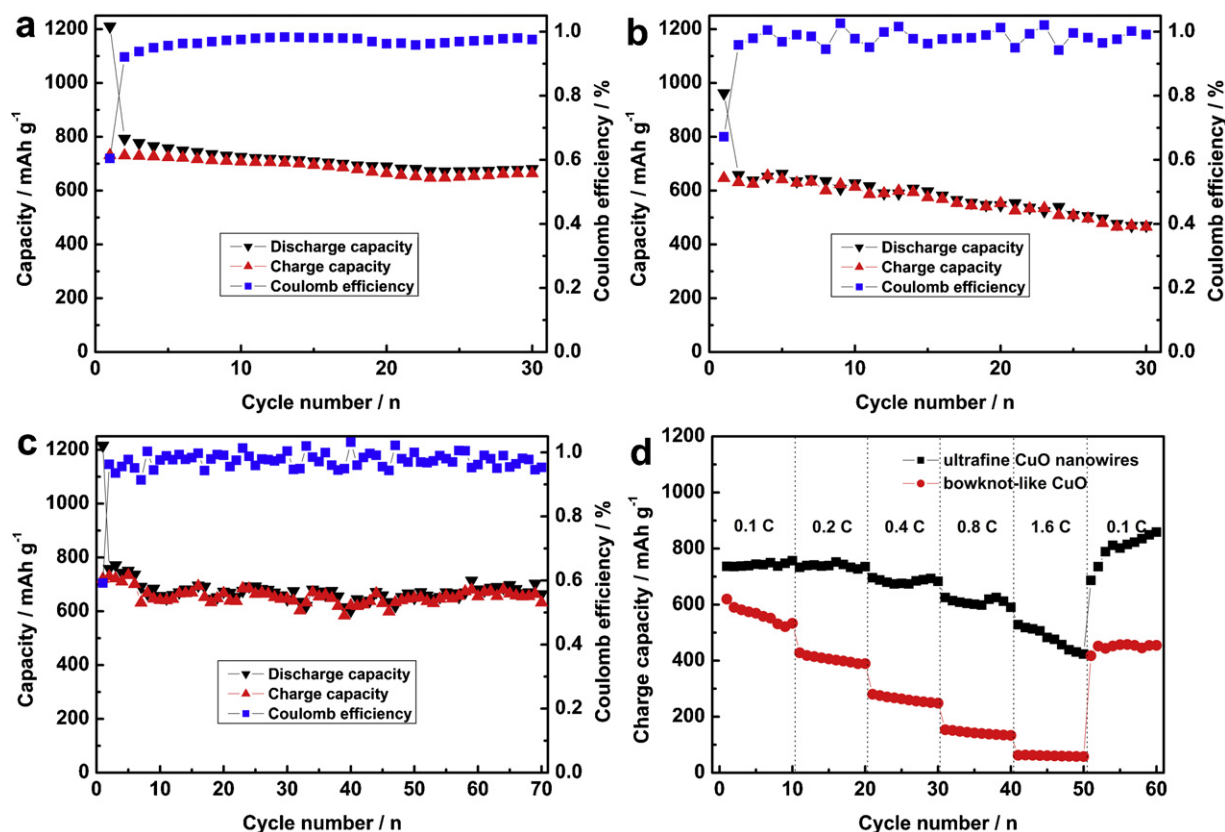


Fig. 6. (a) Cycling performance of ultrafine CuO nanowires at 0.1 C; (b) cycling performance of bowknot-like CuO at 0.1 C; (c) cycling performance of ultrafine CuO nanowires at 0.3 C; (d) cycling performances of ultrafine CuO nanowires and bowknot-like CuO at different current densities.

4. Conclusions

The ultrafine CuO nanowires (~5 nm) with good dispersion are successfully synthesized by a simple solution route combined with a heat treatment. Electrochemical studies indicate that the obtained ultrafine CuO nanowires exhibit high capacity, superior cycling performance and improved rate capability. The discharge capacity after 70 cycles can be maintained at about 660 mAh g⁻¹ at 0.3 C. Therefore, synthesizing nanostructures with ultrafine size is an effective way to improve the electrochemical properties of CuO and other transition metal oxides anode materials.

Acknowledgements

This work was supported by National Natural Science Foundation of China (51002117 and 50871081), Specialized Research Fund for the Doctoral Program of Higher Education of China (20100201120049) and Fundamental Research Funds for the Central Universities (0109-08141012, 08143017).

References

- [1] Y. Idota, T. Kubota, A. Matsufuji, Y. Maekawa, T. Miyasaka, *Science* 276 (1997) 1395–1397.
- [2] P. Poizat, S. Laruelle, S. Grugeon, L. Dupont, J.M. Tarascon, *Nature* 407 (2000) 496–499.
- [3] A.S. Arico, P. Bruce, B. Scrosati, J.M. Tarascon, W. Van Schalkwijk, *Nat. Mater.* 4 (2005) 366–377.
- [4] P.G. Bruce, B. Scrosati, J.M. Tarascon, *Angew. Chem. Int. Ed.* 47 (2008) 2930–2946.

- [5] M.G. Kim, J. Cho, *Adv. Funct. Mater.* 19 (2009) 1497–1514.
- [6] R. Liu, J. Duay, S.B. Lee, *Chem. Commun.* 47 (2011) 1384–1404.
- [7] S.F. Zheng, J.S. Hu, L.S. Zhong, W.G. Song, L.J. Wan, Y.G. Guo, *Chem. Mater.* 20 (2008) 3617–3622.
- [8] B. Wang, X.L. Wu, C.Y. Shu, Y.G. Guo, C.R. Wang, *J. Mater. Chem.* 20 (2010) 10661–10664.
- [9] S. Venkatchalam, H.W. Zhu, C. Masarapu, K.H. Hung, Z. Liu, K. Suenaga, B.Q. Wei, *ACS Nano* 3 (2009) 2177–2184.
- [10] J.Y. Xiang, J.P. Tu, Y.F. Yuan, X.L. Wang, X.H. Huang, Z.Y. Zeng, *Electrochim. Acta* 54 (2009) 1160–1165.
- [11] J.Y. Xiang, J.P. Tu, J. Zhang, J. Zhong, D. Zhang, J.P. Cheng, *Electrochem. Commun.* 12 (2010) 1103–1107.
- [12] C. Li, W. Wei, S.M. Fang, H.X. Wang, Y. Zhang, Y.H. Gui, R.F. Chen, *J. Power Sources* 195 (2010) 2939–2944.
- [13] H.B. Wang, Q.M. Pan, J.W. Zhao, W.T. Chen, *J. Alloys Compd.* 476 (2009) 408–413.
- [14] X.P. Gao, J.L. Bao, G.L. Pan, H.Y. Zhu, P.X. Huang, F. Wu, D.Y. Song, *J. Phys. Chem. B* 108 (2004) 5547–5551.
- [15] L.B. Chen, N. Lu, C.M. Xu, H.C. Yu, T.H. Wang, *Electrochim. Acta* 54 (2009) 4198–4201.
- [16] S.Q. Wang, J.Y. Zhang, C.H. Chen, *Scripta Mater.* 57 (2007) 337–340.
- [17] S.Q. Wang, J.Y. Zhang, N. Ding, C.H. Chen, *Scripta Mater.* 60 (2009) 1117–1120.
- [18] J.C. Park, J. Kim, H. Kwon, H. Song, *Adv. Mater.* 21 (2009) 803–807.
- [19] Q. Pan, H. Jin, H. Wang, G. Yin, *Electrochim. Acta* 53 (2007) 951–956.
- [20] H.B. Wang, Q.M. Pan, H.W. Zhao, G.P. Yin, P.J. Zuo, *J. Power Sources* 167 (2007) 206–211.
- [21] J. Morales, L. Sanchez, F. Martin, J.R. Ramos-Barrado, M. Sanchez, *Electrochim. Acta* 49 (2004) 4589–4597.
- [22] J.Y. Xiang, J.P. Tu, L. Zhang, Y. Zhou, X.L. Wang, S.J. Shi, *J. Power Sources* 195 (2010) 313–319.
- [23] Q.T. Pan, K. Huang, S.B. Ni, F. Yang, S.M. Lin, D.Y. He, *J. Alloys Compd.* 484 (2009) 322–326.
- [24] C.H. Lu, L.M. Qi, J.H. Yang, D.Y. Zhang, N.Z. Wu, J.M. Ma, *J. Phys. Chem. B* 108 (2004) 17825–17831.
- [25] X.J. Zhang, G.F. Wang, X.W. Liu, J.J. Wu, M. Li, J. Gu, H. Liu, B. Fang, *J. Phys. Chem. C* 112 (2008) 16845–16849.
- [26] Z.H. Yang, J. Xu, W.X. Zhang, A.P. Liu, S.P. Tang, *J. Solid State Chem.* 180 (2007) 1390–1396.

- [27] H.L. Xu, W.Z. Wang, W. Zhu, L. Zhou, M.L. Ruan, *Cryst. Growth Des.* 7 (2007) 2720–2724.
- [28] D.P. Singh, A.K. Ojha, O.N. Srivastava, *J. Phys. Chem. C* 113 (2009) 3409–3418.
- [29] X.G. Wen, W.X. Zhang, S.H. Yang, *Nano Lett.* 2 (2002) 1397–1401.
- [30] Y. Cudennec, A. Lecerf, *Solid State Sci.* 5 (2003) 1471–1474.
- [31] Y.J. Zhang, S.W. Or, X.L. Wang, T.Y. Cui, W.B. Cui, Y. Zhang, Z.D. Zhang, *Eur. J. Inorg. Chem.* 16 (2009) 168–173.
- [32] S. Laruelle, S. Grugeon, P. Poizot, M. Dolle, L. Dupont, J.M. Tarascon, *J. Electrochem. Soc.* 149 (2002) A627–A634.
- [33] K.M. Shaju, F. Jiao, A. Débart, P.G. Bruce, *Phys. Chem. Chem. Phys.* 9 (2007) 1837–1842.